Light-pressure-induced nonlinear dispersion of a laser field interacting with an atomic gas

Rudolf Grimm* and Jürgen Mlynek†
Institute of Quantum Electronics, Swiss Federal Institute of Technology, (Eidgenössische Technische Hochschule) Zürich, CH-8093 Zürich, Switzerland
(Received 2 November 1989)

We report on detailed studies of the effect of resonant light pressure on the optical response of an atomic gas to a single monochromatic laser field. In this very elementary situation of laser spectroscopy, the redistribution of atomic velocities that is induced by spontaneous light pressure leads to a novel contribution to the optical dispersion curve of the medium. This light-pressure-induced dispersion phenomenon displays a pronounced nonlinear dependence on the laser intensity. Moreover, for a given intensity, its strength is closely related to the laser beam diameter. As most important feature, this light-pressure-induced dispersion displays an even symmetry with respect to the optical detuning from line center. As a result, the total Doppler-broadened dispersion curve of the gas can become asymmetric, and a significant shift of the dispersion line center can occur. In addition to a detailed theoretical description of the phenomenon, we report on its experimental investigation on the $\lambda = 555.6$ nm $^1S_0$-$^3P_1$ transition in atomic ytterbium vapor with the use of frequency-modulation spectroscopy. The experimental findings are in good quantitative agreement with theoretical predictions.

I. INTRODUCTION

In recent years mechanical effects of light have attracted increasing attention.[1] A variety of experiments has been performed in order to study effects of resonant light forces on the motion of free atoms;[2,3] these forces are induced by the transfer of photon momentum to atoms in resonant interaction processes. So far, most of all experiments on light forces have been performed with the use of atomic beams. It has been shown, e.g., that atomic beams can be strongly deflected and decelerated by laser light;[2] in this context, laser cooling of atoms in a beam is a prominent example.[3]

Resonant light forces, quite obviously, not only affect the velocities of atoms in a beam but also of atoms in a gas.[4,5] So far, very little experimental work has been performed on *light-pressure effects in gases;*[6] here the total modification of the velocity distribution that can be achieved by resonant light pressure under normal experimental conditions seems to be insignificantly small because only few photon momenta can be accumulated by the atoms during their interaction with the laser field. Recent investigations, however, showed that even very small modifications of the atomic velocity distribution can have substantial effects on the *optical response* of a gas to laser light;[7-11] the corresponding effect of light pressure shows up in the transmitted laser light and is manifested in *modifications of absorption and dispersion profiles* with possibly important consequences for high-resolution laser spectroscopy.

The existence of light-pressure-induced phenomena of this kind was first pointed out by Kazantsev, Surdutovich, and Yakovlev, who theoretically investigated the effect of spontaneous light pressure on the nonlinear optical susceptibility of a Doppler-broadened medium.[7] Recent experiments[9-11] concerning two basic situations of laser spectroscopy yielded first experimental verifications of the influence of light pressure on the absorption and dispersion profiles of an atomic gas. On one hand, a light-pressure-induced contribution to the Doppler-broadened dispersion curve of a gas was observed;[9] on the other hand, clear evidence of light-pressure-induced modifications of the Doppler-free resonances in saturation spectroscopy was obtained.[10,11]

In this work, we consider in more detail the effect of resonant light pressure in the very elementary situation of laser spectroscopy where a *single* laser beam interacts with a Doppler-broadened optical transition in an atomic gas [see scheme in Fig. 1(a)]; here spontaneous light pressure can lead to a strong nonlinear contribution to the dispersion of the light field with drastical consequences for the total Doppler-broadened dispersion curve of the medium.[7,8] In extension of previous work,[9] we present a full theoretical description of this phenomenon, and we report on new systematic experimental investigations, which directly allow us to confirm all theoretical predictions.

In our theoretical description (Sec. II) of the effect of light pressure on the optical response of a Doppler-broadened gas of two-level atoms, we show that the velocity redistribution induced by the spontaneous scattering force can substantially affect the *dispersion* of the light field while the absorption remains essentially unchanged. This fact follows from the antisymmetric shape of the light-pressure-induced modification of the velocity distribution with respect to the resonant velocity v_0 [see Fig. 1(b)]. Most importantly, the light-pressure-induced contribution to the Doppler-broadened dispersion curve

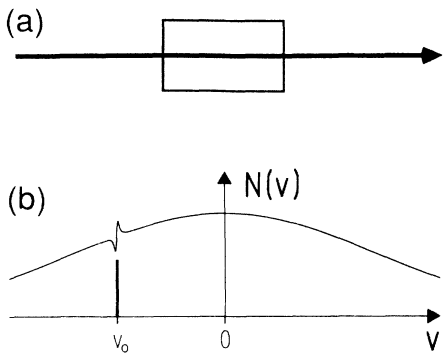

FIG. 1. (a) Scheme of the very elementary situation considered in this work. A single laser beam interacts with the Doppler-broadened transition in an atomic gas. (b) A typical velocity distribution $N(v)$ modified by the resonant light pressure of a monochromatic laser field; here v denotes the atomic velocity component in laser beam direction and v_0 is the resonant velocity determined by the Doppler effect. The antisymmetric modification feature induced in the narrow velocity interval which resonantly interacts with the light field, leads to the light-pressure-induced dispersion phenomenon.

of the medium displays an *even symmetry* with respect to the laser detuning from resonance. This surprising behavior is explained by the fact that the light-pressure-induced dispersion results from a local antisymmetry of the atomic velocity distribution which is induced by the laser light itself in a narrow interval corresponding to the homogeneous optical linewidth [see Fig. 1(b)] and does not exist in the thermal equilibrium distribution. Neither the shape nor the sign of this antisymmetric modification depend on the Doppler detuning of the laser from resonance; the detuning only determines the resonant velocity v_0 where the Doppler distribution is redistributed.

In our experimental studies (Sec. III), we thoroughly investigate the light-pressure-induced dispersion phenomenon in a gas of ytterbium atoms using the technique of frequency-modulation spectroscopy. The measurements reported in this work are obtained on a single Yb isotope in an isotopically pure sample; this medium represents a Doppler-broadened two-level system in an ideal way. Hence our experimental curves directly demonstrate the even symmetry of the light-pressure-induced nonlinear dispersion curve of the medium, in contrast to the more indirect results on natural ytterbium reported previously.[9] The dependence of the dispersion phenomenon on all relevant experimental parameters is studied systematically; we investigate, e.g., its pronounced optical saturation behavior and its dependence on the laser-atom interaction time. Thus the experimental results allow for a direct comparison with our theory, which we now present in Sec. II.

II. THEORY

In our theoretical treatment, we proceed in the following way. First we describe how the resonant light pressure of a single monochromatic laser beam modifies the atomic velocity distribution of a low-pressure gas. Then we evaluate the optical response of the Doppler-broadened medium, and especially consider the effect of the light-pressure-induced velocity redistribution on the corresponding absorption and dispersion curve. Our calculation shows that a substantial modification of the dispersion curve can occur under appropriate conditions. Finally, this light-pressure-induced dispersion phenomenon is discussed in detail.

We model the *atomic medium* as an ensemble of two-level atoms with an inhomogeneously broadened optical transition with frequency Ω and an electric dipole moment μ. We assume that spontaneous emission is the dominant relaxation mechanism for the optical excitation. If $2\Gamma=|\mu|^2\Omega^3/(3\pi\varepsilon_0\hbar c^3)$ (Ref. 12) denotes the spontaneous decay rate of the excited state population, then the corresponding natural linewidth [half width at half maximum (HWHM)] of the optical transition is given by Γ.

The *light field* is described as a monochromatic traveling plane wave with frequency ω and wave number k:

$$E(x,t)=\tfrac{1}{2}\tilde{E}\exp(i\omega t-ikx)+\text{c.c.}\ ; \tag{1}$$

this approximation is justified if the laser beam is not strongly focused and the frequency bandwidth of the laser light is negligibly small compared with the homogeneous optical linewidth of the transition. Because of the Doppler effect the atom-field interaction depends resonantly on the atomic velocity component v in the propagation direction of the light field, with $v_0=(\omega-\Omega)/k$ being the resonant velocity. If the atomic velocity distribution $N(v)$ displays a characteristic width u, the corresponding Doppler width in frequency units is given by ku. We restrict our consideration to the case of a Doppler width ku that is large compared with the natural linewidth Γ; this Doppler limit ($ku\gg\Gamma$) is typical for an optical transition in a low-pressure gas.

A. Modification of the velocity distribution

When an atom is interacting with the light field, cycles of absorption and spontaneous reemission take place; each cycle is connected with an average photon momentum transfer of $\hbar k$ on the atom.[13] For a sufficiently strong optical transition, the Doppler shift $2\varepsilon_r=\hbar k^2/M$ of an atom with mass M due to one photon momentum transfer is small compared with the natural linewidth ($\varepsilon_r\ll\Gamma$). In this case, the effect of photon momentum transfer can be described simply by a force in a classical sense; this well-known spontaneous scattering force[13] is given by

$$F_{\text{sp}}(v)=\hbar k 2\Gamma p(v)\ , \tag{2}$$

with

$$p(v)=\frac{G}{2}\frac{\Gamma^2}{(kv-kv_0)^2+\Gamma^2(1+G)} \tag{3}$$

describing the Lorentzian-shaped excitation probability. Optical saturation is taken into account by the saturation

parameter $G=I/I_{sat}$ in the denominator of Eq. (3). Here $I=\varepsilon_0 c|\tilde{E}|^2/2$ is the intensity of the light field and $I_{sat}=\hbar\Omega^3\Gamma/(6\pi c^2)$ denotes the saturation intensity of the transition.

In order to calculate the modification of the velocity distribution $N(v)$ that is caused by the spontaneous scattering force $F_{sp}(v)$, we consider an atomic ensemble that has an initial velocity distribution $N_0(v)$ and starts to interact with the light field at time $t=0$. The time evolution of the atomic velocity distribution $N(v,t)$ is described by the kinetic equation[14]

$$\frac{\partial}{\partial t}N(v,t)=-\frac{1}{M}\frac{\partial}{\partial v}[F_{sp}(v)N(v,t)] . \tag{4}$$

For a solution of this equation in the Doppler limit ($ku \gg \Gamma$), the initial velocity distribution can be regarded as constant for those atoms that are subjected to light pressure [$N_0(v)=N_0(v_0)$]. If the consideration is furthermore restricted to the case of slight modifications of the velocity distribution, a first-order perturbative treatment of Eq. (4) in time t yields the simple solution

$$N(v,t)=N_0(v)-N_0(v_0)\frac{t}{M}\frac{\partial}{\partial v}F_{sp}(v) . \tag{5}$$

Under stationary conditions, i.e., for a continuous-wave laser excitation, the modified velocity distribution $N(v)$ does not depend explicitly on time. In this case, t has to be replaced in Eq. (5) by an effective interaction time τ (see Appendix A). In this way, using Eqs. (2) and (3) we finally obtain the following expression for the modified velocity distribution:

$$N(v)=N_0(v)+N_{LP}(v) \tag{6a}$$

with

$$N_{LP}(v)=N_0(v_0)\varepsilon_r\tau\frac{4G(kv-kv_0)\Gamma^3}{[(kv-kv_0)^2+\Gamma^2(1+G)]^2} . \tag{6b}$$

Here the light-pressure-induced modification of the velocity distribution is described by $N_{LP}(v)$. The relative strength of the modification is characterized by the ratio of the maximum atomic velocity change $\Delta v=\tau M^{-1}F_{sp}(v_0)$ and the width $k^{-1}\Gamma\sqrt{1+G}$ of the excited velocity interval including saturation broadening. Hence the condition

$$\varepsilon_r\tau\frac{2G}{(1+G)^{3/2}}\ll 1 \tag{7}$$

has to be fulfilled to justify a perturbation approach. In this case, only a slight modification [$|N_{LP}(v)|\ll N_0(v_0)$] of the velocity distribution occurs, and Eq. (6) yields a good approximation.

A typical velocity distribution modified by light pressure is shown in Fig. 1(b). According to Eq. (6), the modification function $N_{LP}(v)$ (see Fig. 2) displays the homogeneous optical linewidth and is completely antisymmetric with respect to $v-v_0$. Let us point out that the Doppler detuning $kv_0=\omega-\Omega$ only determines where the velocity distribution is modified; neither shape nor sign of the antisymmetric modification, however, depend on the detuning from line center. The strength of the modification increases proportionally to G for low intensities ($G\ll 1$) and drops proportionally to $1/\sqrt{G}$ for high intensities ($G\gg 1$); maximum strength is reached for $G=2$.

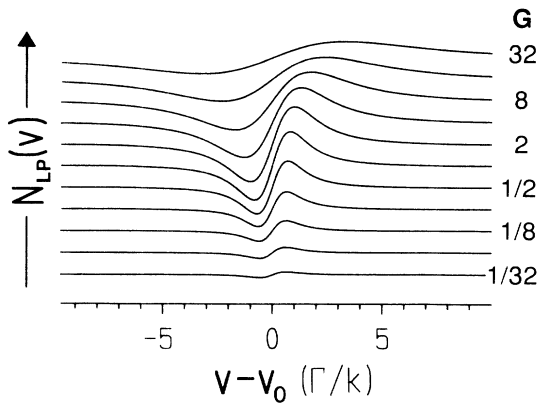

FIG. 2. Typical saturation behavior of the light-pressure-induced modification of the velocity distribution; the corresponding modification function $N_{LP}(v)$ is shown for various optical saturation parameters G. For details see text.

Furthermore, if condition (7) holds, the strength of the modification is proportional to the effective interaction time τ. In an experimental realization on a low-pressure gas, thermalizing collisions within the atomic flight through the laser beam can be neglected; in this case, τ is determined by the transit time of the atoms through the laser beam (see Appendix A), and the strength of the modification of the velocity distribution can be expected to depend linearly on the laser-beam diameter.

B. Calculation of the optical response

After the interaction with the Doppler-broadened medium, the transmitted light can be described as a plane wave analogously to Eq. (1) with the complex amplitude

$$\tilde{E}'=\tilde{E}\exp(-A-iD) , \tag{8}$$

with

$$A=\int_{-\infty}^{+\infty}dv\,N(v)a(v-v_0) , \tag{9a}$$

$$D=\int_{-\infty}^{+\infty}dv\,N(v)d(v-v_0) . \tag{9b}$$

Here the quantities A and D represent the optical response of the medium, i.e., they describe the effects of absorption and dispersion of the sample on the transmitted light of the test beam. A and D are closely related to the absorption coefficient α and the refractive index n by $A=\alpha L/2$ and $D=(n-1)kL$, where L denotes the interaction length within the sample. Our consideration is restricted to the case of an optically thin medium, where A and D are small compared with unity ($A,D\ll 1$).

According to Eqs. (9), A and D are given as ensemble average over all velocities v of the functions $a(v-v_0)$

and $d(v-v_0)$, which, in turn, describe the optical response of a single atomic subgroup of velocity v. With the use of an appropriate density-matrix formalism, the following well-known expressions for $a(v-v_0)$ and $d(v-v_0)$ can be derived:[15]

$$a(v-v_0)=\kappa'\frac{\Gamma}{(kv-kv_0)^2+\Gamma^2(1+G)} , \tag{10a}$$

$$d(v-v_0)=\kappa'\frac{kv-kv_0}{(kv-kv_0)^2+\Gamma^2(1+G)} . \tag{10b}$$

Equations (10a) and (10b) display an absorptive and a dispersive Lorentzian line shape, respectively. The proportionality constant κ' is given by

$$\kappa'=\frac{NkL|\mu|^2}{2\hbar\varepsilon_0} , \tag{11}$$

where N denotes the number density of the gas.

As the total velocity distribution $N(v)$ can be written as sum of the unmodified distribution $N_0(v)$ and the light-pressure-induced modification $N_{\mathrm{LP}}(v)$ [see Eq. (6a)], the total optical response of the Doppler-broadened medium according to Eqs. (9) can be also written as sum of two corresponding contributions: an ordinary part and a light-pressure-induced part [$A=A_0+A_{\mathrm{LP}}$, $D=D_0+D_{\mathrm{LP}}$]. In the following, we calculate and discuss first the ordinary absorption A_0 and dispersion D_0 and then the light-pressure-induced contributions A_{LP} and D_{LP}.

1. Ordinary optical response

With the use of the unmodified velocity distribution $N_0(v)$, Eqs. (9) and (10) yield the following results for the ordinary absorption A_0 and dispersion D_0 in the Doppler limit ($ku \gg \Gamma$):

$$A_0=\kappa N_0(v_0)\frac{1}{\sqrt{1+G}} , \tag{12a}$$

$$D_0=\frac{\kappa}{\pi}\mathrm{P}\int_{-\infty}^{+\infty}dv\frac{N_0(v)}{v-v_0} , \tag{12b}$$

where P denotes principal value. Here we have introduced the new proportionality constant $\kappa=(\pi/k)\kappa'$. According to Eq. (12a), the *ordinary absorption* A_0 simply reflects the Doppler distribution $N_0(v)$. Furthermore, the absorption A_0 shows the well-known saturation behavior of a Doppler-broadened absorption;[15] in the limit of a low intensity ($G \ll 1$), the linear absorption A_{L} is simply given by

$$A_{\mathrm{L}}=\kappa N_0(v_0) . \tag{13a}$$

The *ordinary dispersion* D_0 cannot be expressed in such a simple way by the velocity distribution $N_0(v)$ as is possible for the absorption A_0 [see Eq. (12)]; this fact is due to the slow asymptotic falloff of the homogeneous dispersion function $d(v-v_0)$ proportional to $(v-v_0)^{-1}$, which means that D_0 is essentially not determined by resonant atoms ($|v-v_0| \lesssim \Gamma$) but by atoms far out off resonance ($|v-v_0| \gg \Gamma$). As a consequence, the specific shape of the total velocity distribution $N_0(v)$ has to be taken into account in order to calculate D_0. As another consequence of the Doppler limit ($ku \gg \Gamma$), the homogeneous optical linewidth $\Gamma\sqrt{1+G}$ contained in the homogeneous dispersion function $d(v-v_0)$ [see Eq. (10b)] is not of importance for the dispersion D_0 of the Doppler-broadened medium. Thus, before carrying out the Doppler integration, one can simply replace $d(v-v_0)$ by $\kappa'/(kv-kv_0)$ [see Eq. (10b)]. In this case, also the saturation parameter G drops out: This means that the ordinary dispersion D_0 in the Doppler limit ($ku \gg \Gamma$) is completely *optically linear*. Even if G considerably exceeds unity, D_0 is essentially equal to the dispersion D_{L} in the low-intensity limit ($G \ll 1$):

$$D_{\mathrm{L}}=D_0 . \tag{13b}$$

Saturation of the optical transition can only lead to a significant nonlinear contribution to the dispersion of a Doppler-broadened medium if the light field is so strong that the saturation-broadened homogeneous linewidth $\Gamma\sqrt{1+G}$ reaches the Doppler width ku ($\sqrt{G} \approx ku/\Gamma$); this case of extreme saturation is omitted in our consideration.

2. Light-pressure-induced optical response

With the use of the modification $N_{\mathrm{LP}}(v)$ of the velocity distribution according to Eq. (6b), Eqs. (9) and (10) yield the following results (A_{LP} and D_{LP} denote the effect of light pressure on absorption and dispersion of a Doppler-broadened medium):

$$A_{\mathrm{LP}}=0 , \tag{14a}$$

$$D_{\mathrm{LP}}=\kappa N_0(v_0)\varepsilon_r\tau\frac{G}{2(1+G)^{3/2}} . \tag{14b}$$

As a result of the Doppler integration, the light-pressure-induced modification $N_{\mathrm{LP}}(v)$ of the velocity distribution does not lead to a contribution to the absorption A in our approach. This fact can be understood by the following symmetry argument. While $N_{\mathrm{LP}}(v)$ shows an *odd* symmetry with respect to $v-v_0$, the homogeneous absorption curve $a(v-v_0)$ displays an *even* symmetry. Hence, after integration over all velocities, the product of these two functions cannot contribute to A.

According to Eq. (14b), the light-pressure-induced modification $N_{\mathrm{LP}}(v)$ of the velocity distribution gives rise to the novel contribution D_{LP} to the total dispersion D. This *light-pressure-induced dispersion* D_{LP} is optically *nonlinear* in contrast to the ordinary linear dispersion D_0. Furthermore, the light-pressure-induced dispersion D_{LP} directly reflects the Doppler distribution $N_0(v)$ and thus displays the same shape as the absorption curve. For the symmetric velocity distribution of a gas [$N_0(-v)=N_0(v)$], the light-pressure-induced dispersion displays an *even symmetry*, standing in pronounced contrast to the odd symmetry behavior that is usually attributed to a dispersion curve. This remarkable property is due to the fact that the light-pressure-induced dispersion

arises from an antisymmetry of the velocity distribution $N(v)$ (see Fig. 2) that is induced by the light itself and does not exist in the thermal equilibrium distribution $N_0(v)$.

The strength of the light-pressure-induced nonlinear dispersion is directly determined by the strength of the modification of the velocity distribution. Hence it also shows the same pronounced saturation behavior: It increases proportional to G for $G \ll 1$, reaches a maximum for $G=2$, and drops proportional to $1/\sqrt{G}$ for $G \gg 1$. Furthermore, for a low-pressure gas, the strength of this phenomenon should depend linearly on the laser beam diameter, which determines the atom-field interaction time.

C. Consequences for the total dispersion curve of a gas

In order to discuss the consequences of the light-pressure-induced dispersion phenomenon, we have to compare it with the ordinary dispersion D_0 according to Eq. (12b). As for this purpose a specific velocity distribution $N_0(v)$ must be considered, we here use the one-dimensional Maxwell-Boltzmann distribution function resulting for a gas in thermal equilibrium:

$$N_0(v)=\frac{1}{\sqrt{\pi}u}\exp(-v^2/u^2)\ ; \tag{15}$$

this velocity distribution $N_0(v)$ displays a Gaussian shape. The width of $N_0(v)$ is determined by the most probable thermal velocity $u=\sqrt{2k_BT/M}$, where T denotes the temperature of the gas and k_B is Boltzmann's constant. Using this distribution function and Eqs. (12b) and (14b), we finally obtain the following expressions for the ordinary dispersion D_0 and the light-pressure-induced dispersion D_{LP} in the Doppler limit ($ku \gg \Gamma$):

$$D_0=-\frac{\kappa}{\sqrt{\pi}u}\mathrm{Im}[w(\delta)]\ , \tag{16a}$$

$$D_{\mathrm{LP}}=\frac{\kappa}{\sqrt{\pi}u}\exp(-\delta^2)\varepsilon_r\tau\frac{G}{2(1+G)^{3/2}}\ . \tag{16b}$$

Here, for convenience in the following discussion, we have introduced the dimensionless detuning parameter $\delta=v_0/u$, denoting the laser detuning $kv_0=\omega-\Omega$ in units of the Doppler width ku. In Eq. (16a), D_0 is expressed in terms of the complex function $w(z)$, which is related to the error function by $w(z)=\exp(-z^2)\cdot[1-erf(-iz)]$.[16] For a real argument δ, the imaginary part $\mathrm{Im}[w(\delta)]$ represents the principal value of the convolution integral of a $1/\delta$ function with the Gaussian function $\pi^{-1}\exp(-\delta^2)$; as a consequence, $\mathrm{Im}[w(\delta)]$ and thus also $D_0(\delta)$ are antisymmetric with respect to δ.

The total dispersion curve D and the two different contributions D_0 and D_{LP} according to Eqs. (16) are shown in Fig. 3 for $G=2$ and $\varepsilon_r\tau=1$. Although these parameters, strictly speaking, violate condition (7), our perturbation approach still gives a reasonable result for the light-pressure-induced dispersion; a corresponding comparison with the result of a nonperturbative numerical calculation merely reveals a small quantitative deviation of less than 10%. In the case depicted in Fig. 3, the light-pressure-induced dispersion D_{LP} shows about a third of

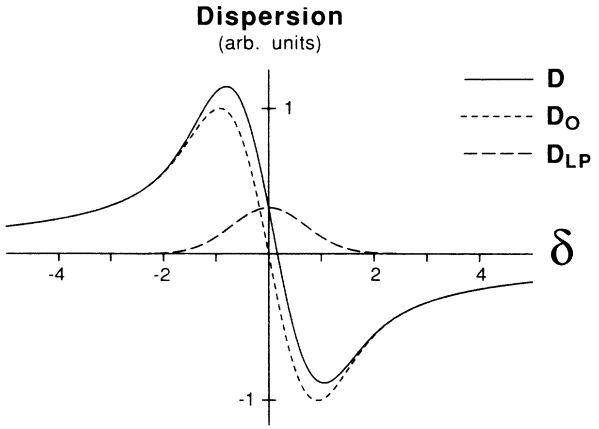

FIG. 3. Theoretical dispersion curves for $\varepsilon_r\tau=1$ and $G=2$: The total dispersion D results as sum of the ordinary linear dispersion D_0 (antisymmetric curve) and the light-pressure-induced contribution D_{LP} (symmetric curve). Here a velocity distribution with a Gaussian shape ($N_0(v)\propto\exp[-(v/u)^2]$) has been assumed; $\delta=(\omega-\Omega)/ku$ denotes the laser detuning in units of the Doppler width.

the maximum strength of the ordinary linear dispersion D_0. The total dispersion curve is asymmetric and its line center displays a significant shift toward higher frequencies; the amount δ_0 of this shift [$D(\delta_0)=0$] can be calculated with the use of the linear expansion $\mathrm{Im}[w(\delta)]\approx 2\delta/\sqrt{\pi}$ (for $|\delta|\ll 1$) from Eqs. (16):

$$\delta_0=\frac{\sqrt{\pi}}{4}\varepsilon_r\tau\frac{G}{(1+G)^{3/2}}\ . \tag{17}$$

For the case depicted in Fig. 3, the frequency shift of zero dispersion amounts to nearly 20% of the Doppler width. Quite obviously, light pressure can have drastic consequences on the dispersion of a Doppler-broadened transition in a low-pressure gas.

D. Higher-order effects

We should mention that spontaneous light pressure can lead to some additional but less important effects on the optical response of a Doppler-broadened medium that are not included in the theoretical approach presented above. For a strong modification of the atomic velocity distribution, i.e., if condition (7) is no longer fulfilled, the solution of the kinetic equation [Eq. (4)] contains substantial higher-order contributions in time t. In this case, the light-pressure-induced dispersion shows a saturation-type behavior with respect to τ. Its strength increases less with τ than in the linear case. In this way, higher-order terms affect the strength of the light-pressure-induced dispersion phenomenon; its dependence on the Doppler detuning $\omega-\Omega$, however, remains unchanged and its even symmetry is not affected.

Furthermore, a strong modification of the velocity distribution also contains a substantial part of even symme-

try with respect to $v-v_0$. This leads to an additional nonlinear contribution to the total absorption. This phenomenon, which occurs in lowest order as second-order contribution proportional to $(\varepsilon_r\tau)^2$, is due to the fact that, for a long interaction time τ, light pressure pushes the atoms out of resonance and thus decreases the number of those atoms that resonantly absorb the light. As this light-pressure effect on the absorption shows an even symmetry with respect to the Doppler detuning $\omega-\Omega$ like the ordinary absorption, shape, and symmetry of the total Doppler-broadened absorption curve are not affected. As a consequence, higher-order effects of light pressure on the absorption are difficult to distinguish from the ordinary saturation of the absorption [see Eq. (12)] and should not play an important role in an experiment.

Moreover, if the limit of a large Doppler width ($ku \gg \Gamma$) is not given, light pressure leads to additional contributions to absorption and dispersion that are in first order proportional to Γ/ku.[7] These contributions may be of importance for the transverse excitation of well-collimated atomic beams with a small residual Doppler width.[17] In a low-pressure gas, however, the Doppler width usually greatly exceeds the homogeneous optical linewidth, and these contributions are negligibly small.

III. EXPERIMENT

Our theoretical study has shown that the light-pressure-induced dispersion phenomenon can occur in the very basic situation of laser spectroscopy where a single laser beam interacts with an atomic gas. Moreover, the dispersion of a light field is a fundamental quantity containing basic information on the atom-field interaction. An explanation that this effect had not been noticed earlier may be given by the fact that dispersion only affects the phase of a light field, which is impossible to observe directly. Nevertheless, an optical phase shift can be detected indirectly by the use of a *phase reference* as is well known, e.g., from optical interferometers, where optical phase information is transformed by interference into observable intensity information.

First we discuss the principle of our experiment to observe the optical phase shift that is caused by the light-pressure-induced dispersion effect. Then the experimental realization is described in detail, and the results of our experiments are presented and discussed.

A. Principle of the experiment

Our experiment to measure the light-pressure-induced dispersion phenomenon is based on *frequency-modulation (FM) spectroscopy*.[18] In this simple and sensitive technique, purely phase-modulated laser light is used to probe the sample. The interaction with the sample gives rise to easily detectable amplitude-modulation components in the transmitted light, which contain the spectroscopic information. Here amplitude modulation occurs not only because of a different absorption of the FM sidebands in the sample but also because of a phase shift of the carrier with respect to the sidebands; in the latter way, the slight phase shift associated with the light-pressure-induced dispersion of a strong carrier can be detected by the use of weak sidebands as a phase reference.

The phase-modulated incident light field can be described by

$$E(x,t)=\tfrac{1}{2}\tilde{E}\exp[i\Phi(t)]\exp(i\omega t-ikx)+\text{c.c.} \tag{18a}$$

with

$$\Phi(t)=m\cos(\omega_M t)\ . \tag{18b}$$

In the case of a weak phase modulation ($m \ll 1$), essentially two sidebands with frequencies $\omega+\omega_M$ and $\omega-\omega_M$ are produced, each having an intensity given by $(m/2)^2$ times the total laser intensity I.

The intensity I' of the transmitted light field can be written in the form

$$I'=I[K-p\cos(\omega_M t)+q\sin(\omega_M t)]\ . \tag{19}$$

In this equation, K is an unmodulated part, p represents the amplitude-modulation component that oscillates in phase with the modulated phase [$\sim\cos(\omega_M t)$], and q denotes the corresponding quadrature modulation [$\sim\sin(\omega_M t)$]. For an *optically thin medium*, the constant part K and the modulation components p and q can be calculated in a simple way:[18]

$$K=1-2A\ , \tag{20a}$$

$$p=m(2D-D_+-D_-)\ , \tag{20b}$$

$$q=m(A_+-A_-)\ . \tag{20c}$$

In these equations, A and D denote the absorption and dispersion of the carrier field and are defined according to Eq. (8). Correspondingly, $A_\pm$ and $D_\pm$ represent the optical response of the medium to upper and lower sideband. Here we assume that the interactions of carrier and sidebands with the medium take place independently; this assumption is justified if the modulation frequency ω_M is large compared with the homogeneous optical linewidth $\Gamma\sqrt{1+G}$, where $G=I/I_{\text{sat}}$ is the saturation parameter of the carrier field.

We furthermore assume that the sideband intensity $(m/2)^2I$ is small compared with the saturation intensity I_{sat} of the optical transition [$(m/2)^2I \ll I_{\text{sat}}$, i.e., $m \ll 2/\sqrt{G}$]; in this case, the interaction of the sidebands with the medium takes place in a completely optically linear way: Hence we write absorption and dispersion of the sidebands in the form

$$A_\pm=A_{\text{L}}(\omega\pm\omega_M)\ , \tag{21a}$$

$$D_\pm=D_{\text{L}}(\omega\pm\omega_M)\ . \tag{21b}$$

We now restrict our consideration to modulation frequencies ω_M that are small compared with the Doppler width ku of the transition; in this case, Eqs. (21a) and (21b) can be expanded linearly in ω_M/ku:

$$A_\pm=A_{\text{L}}(\omega)\pm\omega_M A'_{\text{L}}(\omega)\ , \tag{22a}$$

$$D_\pm=D_{\text{L}}(\omega)\pm\omega_M D'_{\text{L}}(\omega)\ . \tag{22b}$$

Here $A'_L(\omega)=\partial A_L(\omega)/\partial\omega$ and $D'_L(\omega)=\partial D_L(\omega)/\partial\omega$ denote the frequency derivative of the linear absorption and dispersion, respectively. Using Eqs. (22) and (20b), and (20c) and introducing $D_{NL}(\omega)=D(\omega)-D_L(\omega)$ for the nonlinear dispersion of the carrier field, we finally obtain the following expressions for the modulation components p and q:

$$p=2mD_{NL}(\omega)\ , \tag{23a}$$

$$q=2m\omega_M A'_L(\omega)\ . \tag{23b}$$

The in-phase modulation p results from the difference of carrier phase and average phase of the sidebands. In the case of low modulation frequencies ($\omega_M \ll ku$) considered here, the difference in linear dispersion of carrier and sidebands can be neglected, and the in-phase modulation p completely results from the *nonlinear dispersion* D_{NL} of the carrier field [see Eq. (23a)]. For a Doppler-broadened medium, the light-pressure-induced dispersion D_{LP} is the only nonlinear dispersion occurring ($D_{NL}=D_{LP}$). Thus the light-pressure-induced dispersion should directly show up in the in-phase modulation p.

The quadrature modulation q, which occurs as a result of the different absorption of the sidebands [see Eq. (20c)], simply shows the frequency derivative $A'_L(\omega)$ of the *linear absorption* curve. We note that signal contributions arising in this way are well known in frequency-modulation spectroscopy.[18]

The modulation signals that we can expect to measure in an appropriate experiment can be calculated by using Eqs. (23) and the theoretical results obtained in Sec. II:

$$p=\frac{2m\kappa}{\sqrt{\pi}u}\exp(-\delta^2)\varepsilon_r\tau\frac{G}{2(1+G)^{3/2}}\ , \tag{24a}$$

$$q=-\frac{2m\kappa}{\sqrt{\pi}u}\frac{\omega_M}{ku}2\delta\exp(-\delta^2)\ . \tag{24b}$$

Corresponding curves, calculated according to Eqs. (24), are shown in Fig. 4. While the quadrature modulation q does not depend on the laser intensity, the in-phase modulation p directly reflects the pronounced nonlinear behavior of the light-pressure-induced dispersion phenomenon, strongly depending on the optical saturation parameter G.

Our experimental method not only yields direct information on nonlinear dispersion $D_{NL}(\omega)$ and linear absorption $A_L(\omega)$. Indirectly, the linear dispersion curve $D_L(\omega)$ and therewith the total dispersion curve $D(\omega)=D_L(\omega)+D_{NL}(\omega)$ can also be derived from the measured modulation components p and q in the following way. The linear absorption curve can be calculated from $A'_L(\omega)\propto q$ by simple integration:

$$A_L(\omega)=\int_{-\infty}^{\omega}d\omega' A'_L(\omega')\ . \tag{25}$$

Now the well-known Kramers-Kronig relations[19] can be applied to calculate the *linear* dispersion $D_L(\omega)$ from the linear absorption curve $A_L(\omega)$ in the following way:

$$D_L(\omega)=\frac{1}{\pi}\mathrm{P}\int_{-\infty}^{+\infty}d\omega'\frac{A_L(\omega')}{\omega'-\omega}\ . \tag{26}$$

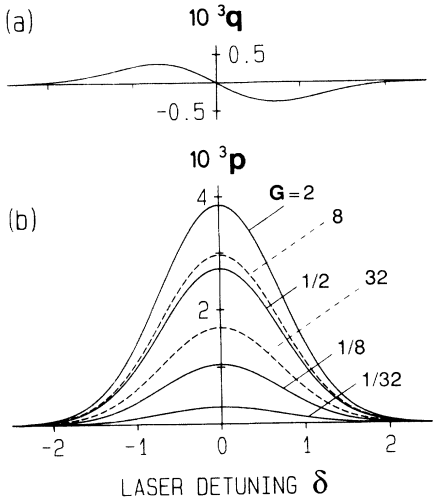

FIG. 4. Calculated quadrature (a) and in-phase (b) components of the amplitude modulation of the transmitted light field for various values of the optical saturation parameter G of the carrier field; here, $\varepsilon_r\tau=1$, $\omega_M/ku=\frac{1}{50}$, $m=\frac{1}{5}$, a Gaussian velocity distribution $N_0(v)\propto\exp[-(v/u)^2]$, and a maximum linear absorption of 10% [$\kappa N_0(0)=0.1$] have been assumed. The quadrature component p directly reflects the light-pressure-induced nonlinear dispersion of the medium.

We note that *linear* absorption and dispersion are, in general, strictly related for an optical medium. If one knows the linear absorption curve of an optical medium, one, in principle, also has full information on the linear dispersion, and vice versa. This strict relation, however, does not apply for the nonlinear optical response of the medium.

Let us summarize the conditions which have to be fulfilled for our experiment. (i) An optically thin medium is required, (ii) the modulation depth of the applied phase-modulation must be sufficiently low to fulfill both

$$m\ll 1 \tag{27a}$$

and

$$m\ll 2/\sqrt{G}\ , \tag{27b}$$

and (iii) the modulation frequency ω_M has to be large compared with the homogeneous optical linewidth $\Gamma\sqrt{1+G}$ but small compared with the Doppler width ku:

$$\Gamma\sqrt{1+G}\ll\omega_M\ll ku\ . \tag{28}$$

The latter condition is illustrated by the frequency scheme of the experiment in Fig. 5(a).

If these conditions are satisfied, our experimental method should allow for a direct observation of the light-pressure-induced dispersion phenomenon; moreover, full information on the total dispersion curve $D(\omega)$ can be obtained in a relatively simple way.

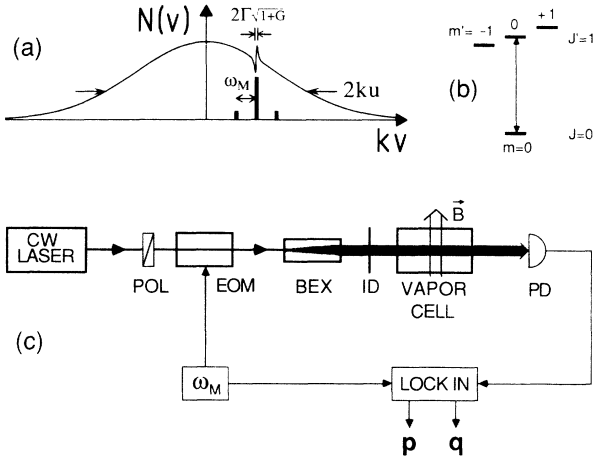

FIG. 5. (a) Schematic of the frequency modulated laser field interacting with the Doppler-broadened medium: The modulation frequency ω_M is small compared with the Doppler width ku but large compared with the homogeneous linewidth $\Gamma\sqrt{1+G}$, and the sidebands are sufficiently weak so that they do not modify the atomic velocity distribution $N(v)$. (b) Scheme of the transition $^1S_0$-$^3P_1$ in atomic ytterbium; excited with π light ($m=0\rightarrow m'=0$), the atoms can be regarded as closed two-level system. (c) Experimental scheme: POL, polarizer; EOM, electro-optical modulator; BEX, beam expander; ID, iris diaphragm; **B** static transverse magnetic field; PD, photodetector.

B. Atomic medium and experimental arrangement

In order to measure the light-pressure-induced dispersion phenomenon, an atomic medium is required that allows to satisfy the conditions for both a strong occurrence of the phenomenon and for the applicability of the experimental method discussed in the previous section. Here atomic ytterbium vapor was found to offer a transition that embodies all requirements in a nearly ideal way.

Our measurements were performed on the line $\lambda=555.65$ nm ($4f^{14}6s^2\,{}^1S_0$-$4f^{14}6s6p\,{}^3P_1$) of ytterbium with mass number 172; a scheme of this $J=0\rightarrow J'=1$ transition is depicted in Fig. 5(b). As the various isotopes contained in natural ytterbium show different isotopic shifts and hyperfine splittings[20] (see also Sec. II C 5), we used isotopically enriched ^{172}Yb for our measurements. Our sample contained 92.5 wt. % of ^{172}Yb and impurities of ^{174}Yb (2.0%), ^{173}Yb (4.5%), and ^{171}Yb (1%); the latter, odd isotopes do not interfere with our measurements since their lines do not overlap the ^{172}Yb line. The Yb vapor was contained in a heated ceramic tube of 1.8-cm diameter; here the length of the heated zone was approximately 6 cm. The temperature of the vapor cell was 830 ± 30 K with a resulting most probable atomic velocity $u=283\pm5$ m/s in thermal equilibrium. The total Yb number density was estimated to be 10^{11} cm^{-3} with a corresponding vapor pressure of roughly 10^{-5} mbar. The natural linewidth of the transition is $\Gamma=2\pi\times96\pm5$ kHz;[21] in our experiment, the Doppler width was $ku=2\pi u/\lambda=2\pi\times510\pm10$ MHz. The saturation intensity of the transition is given by $I_{\rm sat}=2\pi hc\Gamma/(3\lambda^3)=147\pm7$ μW/cm^2. One photon momentum transfer on an ytterbium atom leads to a Doppler shift $2\varepsilon_r=2\pi h/(\lambda^2 M)=2\pi\times7.5$ kHz, corresponding to $\varepsilon_r\approx\Gamma/13$. We note that, if excited with light of appropriate polarization, this ^{172}Yb transition represents a closed two-level system as considered in our theoretical approach.

The simple setup of our experiment is shown in Fig. 5(c). As a tunable light source, we used a continuous-wave single-mode dye ring laser (Spectra Physics 380D); its bandwidth was about 500 kHz (rms) within 5 seconds. The laser light was phase modulated by an electro-optic modulator (Lasermetrics 1039B) with a fixed modulation frequency $\omega_M\approx2\pi\times9.8$ MHz. For this choice, condition (28) is well satisfied ($\omega_M/\Gamma\approx100$, $\omega_M/ku\approx\frac{1}{50}$) in a wide range of laser intensities ($G\lesssim100$). In experiments with moderate laser intensities ($G\lesssim1$), we chose a modulation depth of $m\approx\frac{1}{5}$; in this case, fulfilling condition (27a), about 1% of the total light intensity is transferred to each of the two sidebands. In experiments using high laser intensities ($G\gg1$), even lower modulation depths ($m\approx\frac{1}{10},\frac{1}{20}$) were used in order to satisfy condition (27b). In most of our experiments, the laser beam with a Gaussian profile was expanded to a $1/e^2$ diameter of $d\approx1.3$ cm. In this case, the effective interaction time, approximated by $\tau=\pi d/(4u)$ (see Appendix A), is $\tau\approx35$ μs, corresponding to $\varepsilon_r\tau\approx0.85$; this parameter value turned out to be sufficiently large for a strong occurrence of the light-pressure-induced dispersion phenomenon. The expanded beam was carefully collimated to better than ±0.5 mrad in order to obtain plane wave fronts within the sample. The laser light was linearly polarized parallel to a static transverse magnetic field of roughly 0.3 mT, which lifted the Zeeman-sublevel degeneracy of the transition [see Fig. 5(b)]; hereby well-defined conditions are assured for an exclusive excitation of the optical π transition ($m=0\rightarrow m'=0$). The maximum small-signal absorption of the light within the vapor was less than 10%, so that the condition of an optically thin medium, which was considered theoretically, is realized in our experiment; we note that this also assures that propagation effects within the sample like, e.g., self-focusing and defocusing[22] cannot play any role in the signal formation. After the interaction with the medium, the resulting amplitude modulation of the transmitted light was detected by a fast photodiode. The detector output was demodulated by a high-frequency lock-in amplifier (Princeton 5202), yielding both the in-phase and quadrature amplitude-modulation components p and q, respectively.

C. Experimental results

In this section, we report on our experimental results. First, we present typical measured modulation signals and corresponding dispersion curves, which clearly demonstrate the occurrence of the light-pressure-induced dispersion phenomenon. After that, we discuss experi-

mental series obtained by varying the relevant experimental parameters, i.e., laser intensity and beam diameter. Furthermore, we report on experiments performed with a buffer gas added to the ytterbium vapor, and we discuss measurements obtained on natural ytterbium, demonstrating the effect of optical pumping in other transition schemes. Our experimental results allow a detailed comparison with theory.

1. Typical measured curves

Typical measured modulation signals p and q are shown in Fig. 6 as a function of the laser detuning from line center. These curves clearly display the symmetry behavior that is expected theoretically (see Fig. 4): The quadrature signal q is essentially antisymmetric, and its shape can be understood as derivative of the Doppler profile [see Eq. (24b)]. The in-phase component p shows a relatively strong symmetric signal, which according to Eqs. (24a) and (23a) may be directly interpreted as the nonlinear dispersion of the medium. This nonlinear dispersion apparently reflects the Doppler distribution as expected for the light-pressure-induced dispersion phenomenon. We note that the slight asymmetry which is weakly visible on the left-hand side of the modulation signals in Fig. 6 is caused by the impurity of our ytterbium vapor by the isotope ^{174}Yb.

From the measured modulation signals shown in Fig. 6, we calculated the total dispersion curve of the medium, which results as a sum of the linear dispersion D_L and the nonlinear dispersion D_{NL} ($D=D_L+D_{NL}$); corresponding curves are shown in Fig. 7. Here the nonlinear dispersion curve D_{NL} directly follows from the in-phase component p [see Eq. (23a)], and the linear dispersion D_L is calculated with the use of Eqs. (23b), (25), and (26) from the quadrature modulation q. According to our theoretical consideration, the observed linear dispersion D_L may be identified with the calculated ordinary dispersion D_0 ($D_L=D_0$), resulting from the unmodified velocity distribution [see Eq. (12b)]; moreover, the nonlinear dispersion D_{NL} should be completely determined by the light-pressure-induced dispersion D_{LP} ($D_{NL}=D_{LP}$). This expectation is confirmed by a comparison of experimental (see Fig. 7) with theoretical dispersion curves (see Fig. 3). The observed nonlinear dispersion, in fact, displays the even symmetry that was predicted for the light-pressure-induced dispersion. In further agreement with theoretical expectations,the total dispersion curve shows an asymmetric shape and the frequency of zero dispersion displays a significant shift toward higher frequencies. In the experimental curves shown in Fig. 7, this frequency shift amounts to 32 ± 1 MHz, corresponding to about 6.2% of the Doppler width and more than 300 times the natural linewidth. A more quantitative comparison with theory reveals that this observed frequency shift is weaker than the corresponding theoretical value of 11.2% of the Doppler width, resulting from Eq. (17). This quantitative discrepancy, which means that the light-pressure-induced dispersion phenomenon occurs somewhat weaker than expected, will be considered in more detail in Sec. III C 2.

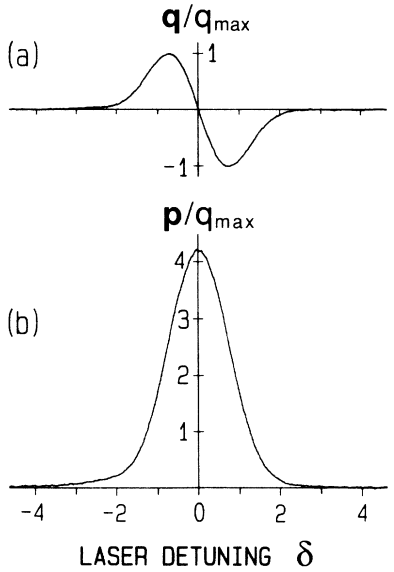

FIG. 6. Typical measured quadrature (a) and in-phase (b) modulation signals q and p, normalized to the maximum signal q_{max} in q. In this example, the laser intensity was 1.2 mW/cm^2, corresponding to $G=8$ and a beam diameter of 1.3 cm ($\varepsilon,\tau\approx0.85$) was used. $\delta=(\omega-\Omega)/ku$ denotes the laser detuning from line center in units of the Doppler width $ku=2\pi\times510$ MHz.

2. Variation of laser intensity

In a series of experiments, we studied the modulation signals for laser intensities from 5 μW/cm^2 to 50 mW/cm^2, covering a range from far below ($G\approx\frac{1}{30}$) to far

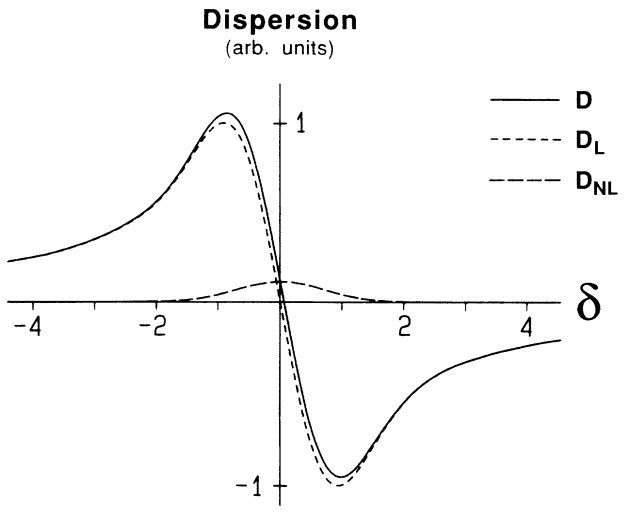

FIG. 7. Experimental dispersion curves, derived from the measured modulation signals shown in Fig. 6. The total dispersion D is given as sum of the linear dispersion D_L and the nonlinear dispersion D_{NL}; the latter is determined by the light-pressure-induced dispersion effect. For details see text.

above saturation ($G \approx 330$). The average number of the cycles of absorption and spontaneous emission that occur for a resonant atom during the interaction time τ is given by $\tau\Gamma G/(G+1)$. Thus, in the range of intensities we used, the average number of photon momenta transferred to resonant ytterbium atoms varies from about 0.7 to 20.

In our experiments, the laser intensity did not affect neither the shape of the modulation signals with respect to the Doppler detuning $\omega-\Omega$ nor the strength of the quadrature signal q, in full accordance with theory. We also confirmed the pronounced intensity dependence of the in-phase component p that is expected for the light-pressure-induced nonlinear dispersion effect. The observed strength $\hat{p}$ of the in-phase signal as a function of the laser intensity is depicted in Fig. 8; this quantity $\hat{p}$ is defined as maximum strength of the in-phase signal p normalized to the corresponding maximum strength of the quadrature signal q ($\hat{p}=p_{\max}/q_{\max}$, see scale in Fig. 6). We note that the experimental data depicted in Fig. 8 refer to the laser intensity in the center of the beam; it turns out that the transverse variation of laser intensity which is due to the Gaussian beam profile only plays a minor role in our experiment (see Appendix A). For a comparison with theory, the solid line in Fig. 8 shows the signal strength $\hat{p}$ that is theoretically expected according to Eqs. (24). Our measurements clearly show the qualitative behavior that is predicted for the light-pressure-induced dispersion. $\hat{p}$ increases linearly for low intensities, reaches a maximum, and decreases for high intensities. A satisfying quantitative agreement with theory, however, only exists for high laser intensities; for low intensities, the observed light-pressure-induced signal is about 6 to 7 times weaker than predicted.

A more detailed consideration (see Appendix B) shows that this quantitative discrepancy of experimental and theoretical results can be sufficiently explained by the short-term frequency jitter of our dye laser occurring within the transit time of the atoms through the laser beam. For low intensities, the corresponding laser bandwidth exceeds the homogeneous linewidth Γ of the transition; as a consequence, the light-pressure-induced modification of the velocity distribution is spread among a wider velocity subgroup than $2\Gamma/k$. This leads to a less pronounced modification compared with monochromatic excitation and thus to a decrease of the corresponding dispersion signal. For sufficiently high intensities, however, saturation broadens the homogeneous optical linewidth $\Gamma\sqrt{1+G}$ so that it exceeds the bandwidth of the laser frequency jitter; in this case, the laser light can be considered as sufficiently monochromatic to be in accordance with the conditions of our theory. As discussed in Appendix B, the laser frequency jitter can be properly taken into account using a simple model in an extended theory. A corresponding curve, which is shown as dashed line in Fig. 8, shows a satisfying agreement with our experimental results. Here a jitter bandwidth of about 230 kHz yields a best fit to the experimental data; without going into detail here, we note that our measurements of the relevant jitter bandwidth showed that this value is quite realistic for the dye laser we used.

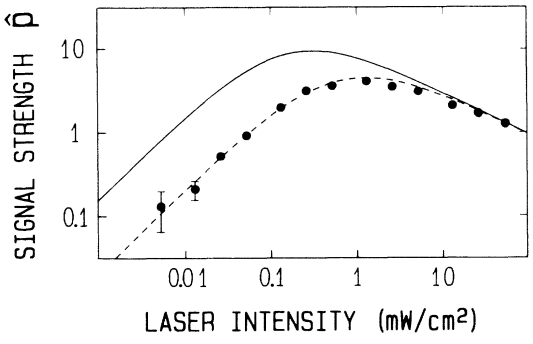

FIG. 8. The measured strength $\hat{p}$ of the light-pressure-induced dispersion signal as a function of the laser intensity; the laser beam diameter was 1.3 cm ($\varepsilon,\tau \approx 0.85$). For a comparison with theory, the solid curve shows the calculated signal strength according to Eq. (24); the dashed curve results from a theory that takes into account a laser frequency jitter with a bandwidth of 230 kHz.

3. *Variation of beam diameter*

As a result of our theoretical consideration, we expect a close relation of the strength of the light-pressure-induced dispersion phenomenon to the laser beam diameter; for the low vapor pressure in our experiment, the laser beam should directly determine the effective interaction time τ of the atoms with the light field, which, in this case, simply results from the transit times of the atoms through the laser beam (see Appendix A). Under the conditions of our experiment, the strength of the light-pressure-induced dispersion phenomenon should depend linearly on the laser beam diameter.

In order to measure the strength $\hat{p}$ of the light-pressure-induced dispersion phenomenon as a function of the laser beam diameter for a constant laser intensity, the laser beam was expanded to a $1/e^2$ diameter of about 2.5 cm and thereafter reduced to various beam diameters

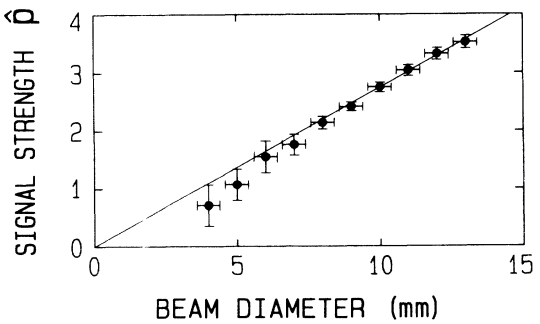

FIG. 9. The observed strength $\hat{p}$ of the light-pressure-induced dispersion signal as a function of the laser beam diameter; the laser intensity of 1.2 mW/cm^2 ($G=8$) is kept constant. The solid line shows a linear fit to the measured values.

from 4 to 13 mm by the use of an iris diaphragm [ID in Fig. 5(b)]; in this series of experiments, the profile of the reduced beam behind the diaphragm was essentially rectangular. The observed dependence of the signal strength $\hat{p}$ on the laser beam diameter is displayed in Fig. 9. In accordance with theory, $\hat{p}$ shows the expected linear behavior. We note that a weak systematic deviation occurs for small beam diameters (see measured values for 4 and 5 mm); this discrepancy is probably due to the fact that diffraction from the iris diaphragm perturbs the planeness of the wave fronts within the sample. Therefore measurements with a small diameter of the diaphragm are not displayed in Fig. 9 as the plane wave approximation is violated.

4. *Addition of a buffer gas: Effect of collisions*

The collision-free regime of a low-pressure gas is one important condition for a strong occurrence of the light-pressure-induced dispersion phenomenon. If this condition is not fulfilled, velocity-changing collisions lead to a rapid thermalization of the velocity distribution, preventing the formation of a substantial light-pressure-induced modification of the velocity distribution. In order to check this expectation, we added small amounts of rare-gas perturber atoms (Ar,He) to the ytterbium vapor. As demonstrated by Fig. 10 for both argon and helium, we observed a clear decrease of the light-pressure-induced dispersion signal for pressures larger than about 10^{-3} mbar.

This observed pressure dependence may be compared with a simple hard-sphere collision model,[23] which yields a pressure of $\sim 10^{-2}$ mbar for the occurrence of one Yb-Ar collision during the effective interaction time τ; the corresponding pressure for one Yb-He collision is $\sim 5\times 10^{-3}$ mbar. For these values, the experimental data already show a strong decrease of the light-pressure-induced dispersion signal by a factor of about 10. This may be understood by the fact that even collisions connected with slight velocity changes ($\Delta v \ll u$) lead to a substantial thermalization of the narrow modification of the velocity distribution. For collisions of this kind, the scattering cross section is, in fact, much larger than the corresponding hard-sphere value.[23]

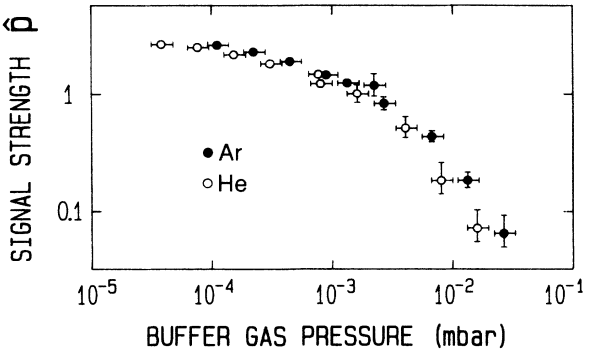

FIG. 10. The measured strength $\hat{p}$ of the light-pressure-induced dispersion signal for various pressures of a buffer gas that was added to the ytterbium vapor; the pressure dependence of $\hat{p}$ was recorded for argon and helium.

5. *Multilevel scheme: Effect of optical pumping*

In multilevel transition schemes, the possible number of photon momenta transferred to the atoms can be strongly limited by optical pumping effects into other levels. Thus a closed transition scheme is an important condition for a strong occurrence of the light-pressure-induced dispersion phenomenon. This fact is demonstrated by the experimental results reported in this section, which we obtained on natural ytterbium.

Natural ytterbium consists of a mixture of seven isotopes with mass numbers 168, 170, 171, 172, 173, 174, and 176. Only the even isotopes, showing no hyperfine splitting because of zero nuclear spin ($I=0$), may be regarded as two-level atoms [see Fig. 11(a)]. For the odd isotopes, however, the nuclear spin (^{171}Yb, $I=\frac{1}{2}$; ^{173}Yb, $I=\frac{5}{2}$) leads to more complicated transition schemes. As a consequence, the ground state ($J=0$) displays a Zeeman substructure and optical pumping between the Zeeman sublevels can occur. As a simple example for the consequences of this effect, let us consider the line $F=\frac{1}{2}\rightarrow F'=\frac{3}{2}$ of ^{171}Yb [see Fig. 11(b)] in the presence of a static magnetic field. Let us assume that the upper $m_F'=-\frac{1}{2}$ Zeeman sublevel is excited by π-polarized laser light interacting resonantly with the $m_F=-\frac{1}{2}\rightarrow m_F'=-\frac{1}{2}$ transition. Spontaneous emission processes lead to the decay of an excited atom to either the $m_F=-\frac{1}{2}$ or the $m_F=\frac{1}{2}$ ground state. If an atom is, in this way, pumped to the $m_F=\frac{1}{2}$ ground state, the cyclic interaction with the laser light is interrupted; a resonant absorption of a laser photon is no longer possible since, as a result of the Zeeman splitting, the $m_F=\frac{1}{2}\rightarrow m_F'=\frac{1}{2}$ transition of this atom is not resonant with the laser light. Optical Zeeman pumping of this kind occurs for all transitions of the odd ytterbium isotopes. Therefore, the maximum number of photon momenta that can be transferred to the odd isotopes is strongly limited under the conditions of our experiment, and the formation of a substantial light-pressure-induced

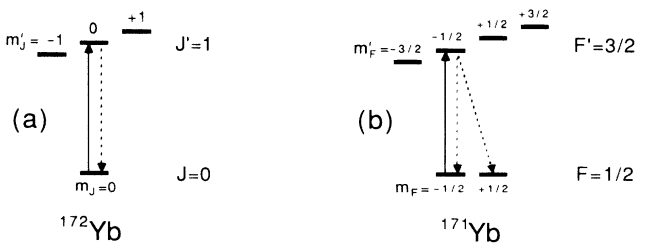

FIG. 11. (a) Scheme of the $J=0\rightarrow J'=1$ transition, occurring in all *even* ytterbium isotope, e.g., ^{172}Yb. (b) Scheme of the transition $F=\frac{1}{2}\rightarrow F'=\frac{3}{2}$ of ^{171}Yb as an example for an *odd* isotope. Absorption and spontaneous emission processes are illustrated by the solid and dashed arrows, respectively.

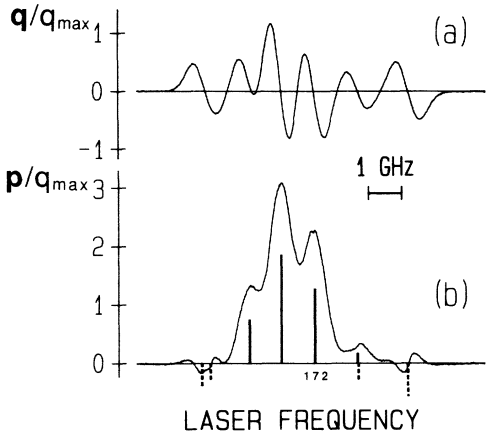

FIG. 12. Typical modulation signals q and p measured on natural ytterbium; q and p are given in units of q_{max} being half the maximum peak to peak value of q. Here the laser intensity was 2.8 mW/cm^2 ($G \approx 20$) and a beam diameter of 1.3 cm ($\varepsilon_r \tau \approx 0.85$) was used. Center frequencies and relative weights of the various even and odd isotopes are illustrated by the solid and dashed bars in (b), respectively. For comparison with Fig. 6, ^{172}Yb is specified particularly.

dispersion is impossible.

Typical modulation signals measured on natural ytterbium are shown in Fig. 12; these curves may be directly compared with corresponding curves obtained on isotopic pure ^{172}Yb. In order to facilitate an interpretation of the measured curves, center frequencies and relative weights[20] of the lines corresponding to the various even and odd isotopes are indicated in Fig. 12(b). As expected [see Eq. (23b)], the quadrature component q shows the derivative of the linear absorption profile; here optical pumping, being a nonlinear process, plays no role and *all* isotopes contribute to the signal according to their relative weights. In contrast, in the in-phase component p, the strong light-pressure-induced signal shows up only for the *even* isotopes. For the odd Yb isotopes, no significant signal occurs; here the residual signals are essentially not due to light pressure. They are related to optical pumping effects between the Zeeman sublevels and occur as a result of the remaining curvature of the wavefronts, leading to a slight frequency sweep that is seen by an atom traversing the beam. In fact, we observed that these residual signals respond in a very sensitive way to the curvature of the wave fronts. Thus, the completely different behavior that shows up in the in-phase modulation p for the even and odd Yb isotopes clearly demonstrates the importance of a closed transition scheme for the occurrence of a strong light-pressure-induced dispersion.

IV. SUMMARY

In this work, we have investigated a novel manifestation of resonant light pressure in a very basic situation of laser spectroscopy. The optical response of an atomic gas to a single monochromatic laser beam can be substantially affected by the small modification of the velocity distribution that is induced by spontaneous light pressure. As a consequence of this modification, the optical dispersion curve of the Doppler-broadened transition can exhibit a strong nonlinear contribution. As the most important feature, this light-pressure-induced nonlinear dispersion shows an *even symmetry* with respect to the Doppler detuning from line center, standing in pronounced contrast to the odd symmetry that is usually attributed to a dispersion curve. As a consequence, the total dispersion curve of the medium can be modified substantially. It becomes asymmetric and the dispersion line center is shifted toward higher frequencies. The strength of the light-pressure-induced dispersion phenomenon displays a pronounced saturation behavior and depends linearly on the atom-field interaction time, which is for a low-pressure gas directly determined by the laser beam diameter. All theoretical expectations are confirmed by our experiments on atomic ytterbium vapor, where we observed the light-pressure-induced dispersion phenomenon with the use of frequency-modulation spectroscopy. Here full quantitative agreement of theoretical and experimental results was achieved by taking the short-term laser frequency jitter into account.

Our work demonstrates that the light-pressure-induced dispersion phenomenon can occur *strongly* if the following conditions are fulfilled: (i) The pressure of the gas must be low to avoid thermalizing collisions, (ii) a relatively wide laser beam has to be used for a sufficiently long interaction time of the atoms with the laser light, and (iii) a closed optical transition scheme is required for a cyclic interaction with the laser photons. We point out that conditions (i) and (ii) are often fulfilled in high-resolution laser spectroscopy in order to prevent collisional and transit-time broadening of spectral lines. With respect to condition (iii), the experimental results suggest that its fulfillment may not be strictly required in some situations. Our measurements demonstrate that even the photon momentum transfer that is connected with only a few cycles of absorption and spontaneous emission can lead to significant line-shape modifications. In fact, we even observed a light-pressure-induced dispersion being due to *less than one* average absorption-emission cycle occurring for an atom that is resonantly excited. Thus phenomena of this kind may also occur under conditions where the number of photon momentum transfers is principally limited, e.g., by optical pumping processes into a third level. Although the effect of the light-pressure-induced dispersion on the measured signals was negligibly small for the specific multilevel system we have investigated (see Sec. III C 5), we point out that related phenomena may generally also occur in more complicated transition schemes than in the basic situation of a two-level system.

Line-shape modifications related to this work have already been observed for the transverse excitation of an atomic beam with a single traveling wave laser field;[17] here slight asymmetries induced by spontaneous light pressure occurred in the power-broadened absorption profile of the laser light. In this experimental situation of

a *homogeneous* medium a corresponding dispersion effect should also occur; it would represent the direct analog to the light-pressure-induced dispersion phenomenon considered in our work for the *inhomogeneously* broadened transition in a gas. In laser spectroscopy, another prominent example for the effect of photon momentum transfer on the atoms in a gas is given by the well-known recoil splitting of the Lamb dip,[24] which can occur for very weak optical transitions as a consequence of the *single* photon momentum transfer that is inherently connected with an absorption process. In contrast to this, the line-shape modifications considered in this work and in Refs. 7–11, 17, and 25 are a result of photon momentum transfer that is connected with cumulative cycles of absorption and spontaneous reemission, leading to the well-known spontaneous scattering force. As a consequence, phenomena of this class can be also present for strong optical transitions.

Possible consequences of the light-pressure-induced dispersion phenomenon investigated in this work may occur in a variety of experimental situations of laser spectroscopy. It may play an important role whenever optically phase-sensitive methods are applied to investigate low-pressure gases; in this respect, various nonlinear spectroscopic techniques using optical heterodyne detection may be mentioned as examples.[26] The light-pressure-induced dispersion may also affect polarization phenomena like, e.g., the well-known Faraday rotation,[27] which can be explained in terms of a different dispersion of the polarization components of a light field. Finally, we note that the optical response of a gas to laser light may be also affected by stimulated light forces if strongly spatially varying fields are used in an experiment, e.g., in an intense standing wave[28,29] or for a laser beam that is strongly focused; so far, however, experimental studies of this type have not been reported for atoms in a gas.

In conclusion, our work shows a very basic example for a novel class of light-pressure-induced phenomena in a low-pressure atomic gas. The induced redistribution of velocities can lead to substantial nonlinear contributions to the optical response of the medium, which are related to a perturbation of the external atomic degrees of freedom. Besides containing basic information on light-matter interaction, light-pressure-induced modifications of spectral lines may be of importance in various situations of high-resolution optical spectroscopy using gas cells.

ACKNOWLEDGMENTS

We are greatly indebted to the late Professor A. P. Kazantsev, who, by his pioneering work, has drawn our attention to the fascinating subject of light forces on atoms.

APPENDIX A: CALCULATION OF THE EFFECTIVE INTERACTION TIME τ

In our theoretical treatment of the light-pressure-induced modification of the velocity distribution (see Sec. II A), the quantity τ was introduced as an effective interaction time of the atoms with the laser field. Here, the calculation of τ for our experimental situation deserves some discussion. For a low-pressure gas, τ is determined by the transit times of the atoms through the laser beam. In order to describe the experimental situation properly, τ must include various effects, i.e., the distribution of transit times, resulting from different transverse velocities and different trajectories, and the fact that, for a Gaussian beam, various light intensities are seen by the atoms traversing the beam. Possible consequences of these effects in laser spectroscopy are discussed, e.g., in Ref. 30.

Here we want to derive a simple approximation to calculate the effective interaction time τ. Let us consider an ensemble of atoms traversing the laser beam and reaching the beam center at time $t=0$. All these atoms experience a Gaussian laser pulse reflecting the beam profile:

$$I(t)=I_0\exp[-(2v_\perp t/d)^2] . \tag{A1}$$

Here d is the laser beam diameter ($1/e$ intensity drop) and $v_\perp$ is the transverse velocity perpendicular to the laser beam. For the large beam diameters we used in our experiments, the intensity varies so slowly that the transient response of the atom to the light can be neglected and the atoms display a steady-state excitation. Let us restrict our consideration to the linear regime of low laser intensities, where the formation of the modification of the velocity distribution depends linearly on both laser intensity and interaction time. In this simple case, the strength of the modification is proportional to the time integral of the intensity $I(t)$ that is seen by the atoms until they reach the center of the beam at $t=0$:

$$\int_{-\infty}^{0} I(t)dt = I_0\frac{\sqrt{\pi}d}{4v_\perp} . \tag{A2}$$

This means that, in the linear regime of low intensities, a Gaussian beam with maximum intensity I_0 and diameter d leads to the same modification of the velocity distribution in the beam center as a rectangular beam with constant intensity I_0 and diameter $\sqrt{\pi}d/2$. Thus, according to Eq. (A2), we can neglect the spatial intensity variation, considering a constant laser intensity I_0 and an interaction time $\sqrt{\pi}d/(4v_\perp)$ for the atoms of transverse velocity $v_\perp$. The velocity average of this time yields the effective interaction time τ:

$$\tau=\int_0^\infty dv_\perp w(v_\perp)\frac{\sqrt{\pi}d}{4v_\perp} . \tag{A3}$$

Here the distribution function of transverse velocities, following from two-dimensional Maxwell-Boltzmann statistics, is given by

$$w(v_\perp)=2v_\perp/u^2\exp(-v_\perp^2/u^2) . \tag{A4}$$

By the use of Eqs. (A3) and (A4), we finally obtain

$$\tau=\frac{\pi d}{4u} . \tag{A5}$$

We point out that this result, which has been derived considering atoms in the center of the beam in the linear regime of low intensities, is strictly justified for an experimental situation where the atoms are probed only in the

center of the beam and where low laser intensities ($G \ll 1$) are used.[10,11]

For the experiment reported here, the situation is much more complicated also because atoms being not in the center of the beam contribute to the measured signals; moreover, high laser intensities ($G \gg 1$) were used in a part of the experiments. For this situation a rigorous calculation of τ seems to require a rather extensive theoretical treatment. Instead of this inconvenient way, we experimentally studied the consequences of both the atoms being not in the center of the beam and the spatial variation of the laser intensity for the measured signals. In a first series of experiments using a diaphragm behind the sample, we compared the signals resulting from the center of the beam with the corresponding signals resulting from the total Gaussian beam. For all intensities from far below to far above saturation, only insignificant quantitative deviations occurred. The relative strength $\hat{p}$ of the light-pressure-induced dispersion signal showed small differences within $\pm 10\%$. In another series of experiments, we compared the signals resulting from a Gaussian beam with corresponding signals obtained by a laser beam with rectangular beam profile. These experiments confirmed that a Gaussian beam with a maximum intensity I_0 and $1/e^2$ diameter d leads to essentially the same modulation signals as a rectangular beam with a constant intensity I_0 and diameter $\sqrt{\pi}\,d/2$ [see Eq. (A2)]; even for high laser intensities, this agreement was still good. In all cases, quantitative deviations of the observed relative strength $\hat{p}$ of the light-pressure-induced dispersion signal did not exceed $\pm 10\%$. All these experimental findings indicate that our simple approach to calculate the effective interaction time τ [see Eq. (A5)] yields a fairly good approximation for all cases in our experiment. This is also confirmed by the fact that with the use of this simple approximation for τ we could achieve a satisfying agreement of theoretical and experimental results (see Sec. III C).

APPENDIX B: EXTENDED THEORY TAKING LASER FREQUENCY JITTER INTO ACCOUNT

In our theoretical treatment presented in Sec. II, we have considered the light field as being perfectly monochromatic. This assumption properly describes the experimental situation, if the laser bandwidth is small compared with the homogeneous optical linewidth Γ; thus, for the ytterbium transition ($\Gamma \approx 2\pi \times 100$ kHz) investigated in this work, laser frequency stabilization to better than 100 kHz would be required to directly compare theoretical and experimental results. The dye laser we used in our experiments, however, did not fully meet this requirement. As a consequence, theoretical and experimental results do not show a full quantitative agreement. In order to remove this discrepancy, we present here an extended theory that takes into account the frequency jitter in a simple theoretical model, where the effect of the jitter is included in the modified velocity distribution.

In our experiment two different time scales are relevant. For the optical excitation, the characteristic time is given by the lifetime $1/(2\Gamma) \approx 830$ ns of the excited state population, and for the formation of the modification of the velocity distribution, the effective interaction time $\tau \approx 35$ μs is significant. Thus, the optical excitation only reacts on relatively fast frequency jitter occurring within 830 ns, i.e., spectral components of the laser noise with relatively high frequencies. In contrast to this, the velocity distribution is also affected by relatively slow jitter within 35 μs, i.e., spectral components of the laser noise with relatively low frequencies. As the typical noise spectrum of a dye laser shows a strong decrease of the noise amplitude with increasing frequency,[31] we can expect that the laser frequency jitter plays a much more important role for the light-pressure-induced modification of the atomic velocity distribution than for the optical excitation. Therefore, in our simple theoretical model, we neglect the effect of laser frequency jitter on the optical excitation, restricting our consideration to its effect on the modified velocity distribution.

As a consequence of the laser frequency jitter, the light-pressure-induced redistribution of atomic velocities takes place in a wider velocity subgroup than in the case of monochromatic light, and the modification feature becomes wider and weaker. In our case, the laser frequency jitter may be interpreted as mechanism leading to an additional broadening of the modification being stochastically independent of the spontaneous decay. Thus, in our simple model, we introduce an effective jitter bandwidth γ and include the effect of jitter in the modification of the velocity distribution in the following way. We simply extend Eq. (6b), which describes the modification for mono-

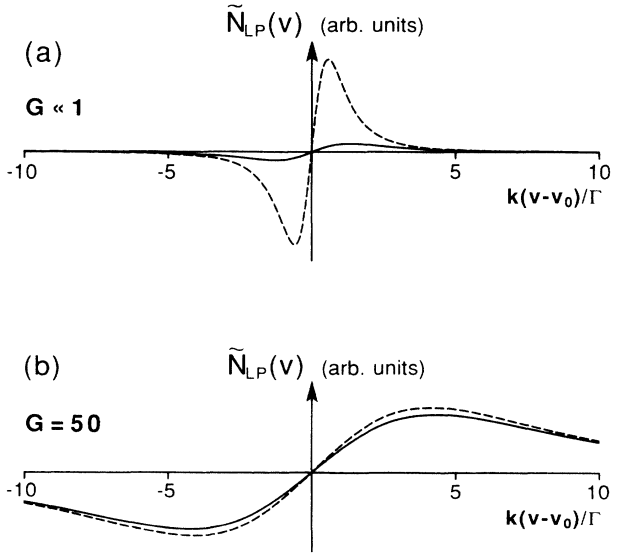

FIG. 13. The solid curves depict the modification of the velocity distribution that is induced by nonmonochromatic laser light with an effective frequency bandwidth $\gamma = 2\Gamma$ (a) in the limit of low laser intensity ($G \ll 1$), and (b) for a high laser intensity ($G = 50$). For comparison, the dashed curves show the corresponding modifications caused by monochromatic light ($\gamma = 0$).

chromatic light, by introducing a phenomenological broadening term γ^2 in the denominator of this equation:

$$\tilde{N}_{\mathrm{LP}}(v)=N_0(v_0)\varepsilon_r\tau\frac{4G(kv-kv_0)\Gamma^3}{[(kv-kv_0)^2+\Gamma^2(1+G)+\gamma^2]^2}\ . \tag{B1}$$

A quadratic term like this γ^2 usually results from a stochastically independent process. The typical behavior of the modification $\tilde{N}_{\mathrm{LP}}(v)$ resulting from this equation is demonstrated in Figs. 13(a) and 13(b). For low intensities, the modification is strongly affected by the jitter [see Fig. 13(a)]. In contrast to this, for sufficiently high intensities, the saturation broadening of the homogeneous linewidth exceeds the jitter bandwidth, and the effect of the jitter on the modification becomes negligibly small [see Fig. 13(b)].

Thus, our theoretical model yields a relatively simple possibility to calculate the light-pressure-induced dispersion $\tilde{D}_{\mathrm{LP}}$ including the effect of laser frequency jitter by using Eq. (B1) instead of Eq. (6b) for the modification of the velocity distribution. In this way, we obtain $\tilde{D}_{\mathrm{LP}}$ according to Eq. (2.9b):

$$\tilde{D}_{\mathrm{LP}}=\int_{-\infty}^{+\infty}dv\,\tilde{N}_{\mathrm{LP}}(v)d(v-v_0)\ . \tag{B2}$$

We note that, in our simple approach, the homogeneous dispersion function $d(v-v_0)$ is not affected by the frequency jitter. Carrying out the integration (B2), we obtain

$$\tilde{D}_{\mathrm{LP}}=\kappa N_0(v_0)\varepsilon_r\tau\frac{2G}{\sqrt{1+G+s}\,(\sqrt{1+G+s}+\sqrt{1+G})^2}\ . \tag{B3}$$

Here the dimensionless jitter parameter $s=(\gamma/\Gamma)^2$ denotes the square of the relevant jitter bandwidth γ normalized to the homogeneous optical linewidth Γ. According to Eq. (B3), the frequency jitter leads to a pronounced decrease of the strength of the light-pressure-induced dispersion if the laser intensity is low ($G\ll s$). For sufficiently high intensities ($G\gg s$), however, the effect of laser frequency jitter is negligibly small since the modification of the velocity distribution is not significantly affected [see Fig. 13(b)].

With the use of Eq. (B3), a satisfying agreement of theory and experimental results can be achieved; this fact is demonstrated by the dashed curve in Fig. 8 resulting from Eq. (B3) with the assumption of an effective jitter bandwidth $\gamma=2.4\Gamma\approx 2\pi\times 230$ kHz. This value, yielding a best fit to experimental data, is confirmed by independent measurements of the relevant jitter bandwidth γ, which we performed with the use of an optical spectrum analyzer (Spectra Physics 470); according to these measurements the relevant jitter bandwidth of our dye laser lies within a range of 150–350 kHz. Thus, our simple theoretical model shows that the effect of laser frequency jitter sufficiently explains the quantitative discrepancy of the theory derived for perfectly monochromatic laser light and our experimental results.

---

*Present address: Max-Planck-Institut für Kernphysik, D-6900 Heidelberg, Federal Republic of Germany.

†Corresponding author, with following present address: Fakultät für Physik, Universität Konstanz, D-7750 Konstanz, Federal Republic of Germany.

[1]See, e.g., J. Opt. Soc. Am. B **2**, 1705 (1985), and references therein (special issue on the mechanical effects of light).

[2]V. G. Minogin and V. S. Letokhov, *Laser Light Pressure on Atoms* (Gordon and Breach, London, 1987), and references therein.

[3]W. Phillips, P. L. Gould, and P. D. Lett, Science **239**, 877 (1988), and references therein.

[4]T. W. Hänsch and A. L. Schawlow, Opt. Commun. **13**, 68 (1975).

[5]J. Dalibard, Opt. Commun. **68**, 203 (1988).

[6]J. H. Xu and L. Moi, Opt. Commun. **67**, 282 (1988).

[7]A. P. Kazantsev, G. I. Surdutovich, and V. P. Yakovlev, Pis'ma Zh. Eksp. Teor. Fiz. **43**, 222 (1986) [JETP Lett. **43**, 281 (1986)], and references therein.

[8]R. Grimm and J. Mlynek, J. Opt. Soc. Am. B **5**, 1655 (1988).

[9]R. Grimm and J. Mlynek, Phys. Rev. Lett. **61**, 2308 (1988).

[10]R. Grimm and J. Mlynek, Phys. Rev. Lett. **63**, 232 (1989).

[11]R. Grimm and J. Mlynek, Appl. Phys. B **49**, 179 (1989).

[12]See, e.g., S. Stenholm, *Foundations of Laser Spectroscopy* (Wiley, New York, 1984), p. 30.

[13]See V. G. Minogin and V. S. Letokhov, Ref. 2, pp. 15–26.

[14]See V. G. Minogin and V. S. Letokhov, Ref. 2, pp. 122–126.

[15]See, e.g., V. S. Letokhov and V. P. Chebotaev, in *Nonlinear Laser Spectroscopy*, Vol. 4 of *Springer Series in Optical Sciences* (Springer, Berlin, 1977), pp. 46–58.

[16]*Handbook of Mathematical Functions*, edited by M. Abramowitz and I. A. Stegun (Dover, New York, 1972), p. 297.

[17]P. R. Hemmer, F. Y. Wu, and S. Ezekiel, Opt. Commun. **38**, 105 (1981).

[18]G. C. Bjorklund, Opt. Lett. **5**, 15 (1980).

[19]See, e.g., A. Yariv, *Quantum Electronics*, 2nd ed. (Wiley, New York, 1975), p. 155.

[20]J. H. Broadhurst *et al.*, J. Phys. B **7**, L513 (1974).

[21]M. Baumann and G. Wandel, Phys. Lett. **22**, 283 (1966).

[22]J. E. Bjorkholm and A. Ashkin, Phys. Rev. Lett. **32**, 129 (1974).

[23]See, e.g., P. R. Berman, in *New Trends in Atomic Physics*, edited by G. Grynberg and R. Stora (North-Holland, Amsterdam, 1984), Vol. 1, p. 451.

[24]A. P. Kol'chenko, S. G. Rautian, and R. I. Sokolovskii, Zh. Eksp. Teor. Phys. **55**, 1864 (1968) [Sov. Phys.—JETP **28**, 986 (1968)]; J. L. Hall, C. J. Bordé, and K. Uehera, Phys. Rev. Lett. **37**, 1339 (1976).

[25]P. R. Hemmer, B. W. Peuse, F. Y. Wu, J. E. Thomas, and S. Ezekiel, Opt. Lett. **6**, 531 (1981).

[26]See, e.g., J. Opt. Soc. Am. B **2**, 1427 (1985) (special issue on ultrasensitive laser spectroscopy); M. D. Levenson and G. L. Eesley, Appl. Phys. **19**, 1 (1979); A. Schenzle, R. G. DeVoe, and R. G. Brewer, Phys. Rev. A **25**, 2606 (1982); R. K. Raj, D. Bloch, J. J. Synder, G. Camy, and M. Ducloy, Phys. Rev.

Lett. **44**, 1251 (1980); G. Camy, C. J. Bordé, and M. Ducloy, Opt. Commun. **41**, 325 (1982); M. Gehrtz, G. C. Bjorklund, and E. A. Whittaker, J. Opt. Soc. Am. B **2**, 1510 (1985); J. Mlynek, R. Grimm, E. Buhr, and V. Jordan, Appl. Phys. B **45**, 77 (1988).

[27]X. Chen, V. L. Telegdi, and A. Weis, J. Phys. B **20**, 5653 (1987), and references therein.

[28]M. G. Prentiss and S. Ezekiel, Phys. Rev. Lett. **56**, 46 (1986).

[29]C. Salomon, J. Dalibard, A. Aspect, H. Metcalf, and C. Cohen-Tannoudji, Phys. Rev. Lett. **59**, 1659 (1987).

[30]C. J. Bordé, J. L. Hall, C. V. Kunasz, and D. G. Hummer, Phys. Rev. A **14**, 236 (1976).

[31]See, e.g., M. Houssin, M. Jardino, B. Gely, and M. Desaintfuscien, Opt. Lett. **13**, 828 (1988), and references therein.

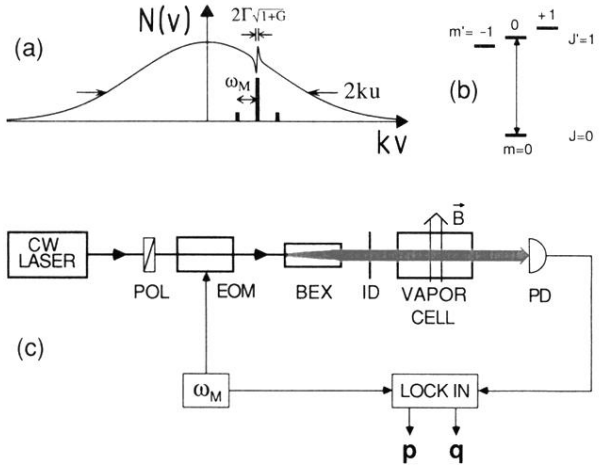

FIG. 5. (a) Schematic of the frequency modulated laser field interacting with the Doppler-broadened medium: The modulation frequency ω_M is small compared with the Doppler width ku but large compared with the homogeneous linewidth $\Gamma\sqrt{1+G}$, and the sidebands are sufficiently weak so that they do not modify the atomic velocity distribution $N(v)$. (b) Scheme of the transition $^1S_0$-$^3P_1$ in atomic ytterbium; excited with π light ($m=0\rightarrow m'=0$), the atoms can be regarded as closed two-level system. (c) Experimental scheme: POL, polarizer; EOM, electro-optical modulator; BEX, beam expander; ID, iris diaphragm; **B** static transverse magnetic field; PD, photodetector.